Supplementary Information

A synthetic lethal interaction between APC/C and topoisomerase poisons uncovered by proteomic screens

Manuel Eguren,[1] Mónica Álvarez-Fernández,[1] Fernando García,[2] Andrés J. López-Contreras,[3] Kazuyuki Fujimitsu,[4] Hiroko Yaguchi,[4] José Luis Luque-García,[5] Oscar Fernández-Capetillo,[3] Javier Muñoz,[2] Hiroyuki Yamano[4] and Marcos Malumbres[1],*

[1] Cell Division and Cancer Group, Spanish National Cancer Research Centre (CNIO) Madrid, E-28029 Spain.

[2] Proteomics Unit, Spanish National Cancer Research Centre (CNIO) Madrid, E-28029 Spain.

[3] Genomic Instability Group, Spanish National Cancer Research Centre (CNIO) Madrid, E-28029 Spain.

[4] Cell Cycle Control Group, University College London Cancer Institute, London, WC1E 6BT U.K.

[5] Dpt. Analytical Chemistry. Complutense University of Madrid, Madrid, E-28015 Spain

Supplementary Experimental Procedures

Proteomic analysis

For SILAC (Ong et al, 2002) analysis, fifty μg of proteins were separated by SDS-PAGE, sliced into 24 pieces and digested with trypsin as described (Shevchenko et al, 2006). Desalted peptides were separated by reversed-phase chromatography (Reprosil-Pur C18 3 μm, 200x 0.075 mm, Dr. Maisch GmbH. Germany), using a nanoLCUltra1D+ system (Eksigent, Dublin CA, USA), directly coupled in line with a LTQ-Orbitrap Velos (Thermo Fisher Scientific, Waltham, USA) via nanoelectrospray source (Thermo Fisher Scientific) (Olsen et al, 2005). Mass spectra were acquired in a data-dependent manner, with an automatic switch between MS and MS/MS scans using a top 15 method. Raw files were analyzed by MaxQuant (version 1.1.1.25) (Cox and Mann, 2008) interrogating the IPI-mouse V3.77 database. Oxidation of methionines, acetylation of protein n-terminus, SILAC-K8 and SILAC-R10 were set as variable modifications, whereas carbamidomethylation of cysteines was set as fixed. Minimal peptide length was set to 6 amino acids and a maximum of two missed-cleavages were allowed. For protein assessment, at least two unique peptides with a FDR <= 1% were required. For quantification purposes, only proteins identified with two or more unique peptides and with two or more SILAC pairs were considered. For iTRAQ, (Ross et al, 2004) assays, raw files were processed by Proteome Discoverer 1.3 (Thermo Scientific). Data were searched by interrogating the Uniprot_Mouse database, comprising both the canonical and manually reviewed isoform sequences (release 2012_09, 50544 entries) using MASCOT (v 2.2) (Perkins et al., 1999) as the search engine. Lysine and peptide N-termini labelling with iTRAQ-4plex reagent as well as carbamidomethylation of cysteine were considered as fixed modifications, while oxidation of methionine was chosen as variable modification for database searching. Both peptide and protein identification were filtered at 1% false discovery rate (FDR) using the target-decoy approach (Elias and Gygi, 2007). The thresholds used to determine proteins being up-regulated were calculated by manual inspection of the data. To this end, ratios were plotted against intensities and a cut-off was chosen based on the distribution of the vast majority of proteins showing no change for each the three analyses. The narrower distributions of the iTRAQ-labelled experiments are due to the compression of ratios associated with this technique.

Supplementary Figures

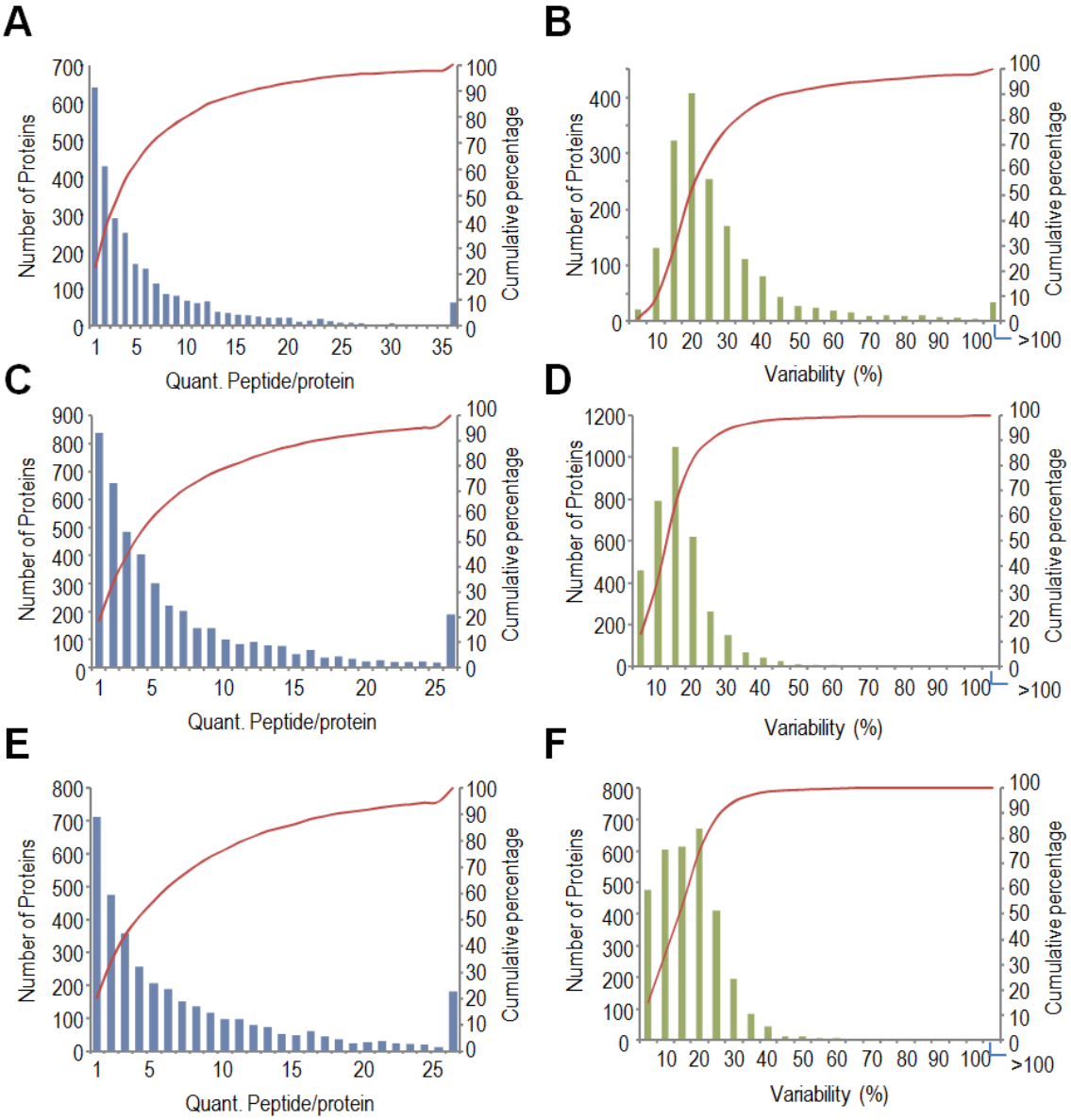

Figure S1. Evaluation of protein quantification quality in the three proteomic screenings (related to Figs. 1 and 2). The number of quantified peptides per protein is shown for A, SILAC-labeled MEFs, C, iTRAQ-labeled serum-starved MEFs and E, iTRAQ-labeled Cdh1-brains. In all three cases, more than 80% of the proteins were quantified on the basis of at least 2 unique peptides. Furthermore, 76-95% of the quantified proteins showed variability levels (i.e. relative standard deviation, RSD) below 30% for B, SILAC-labeled MEFs, D, iTRAQ-labeled serum-starved MEFs and F, iTRAQ-labeled Cdh1-deficient brains.

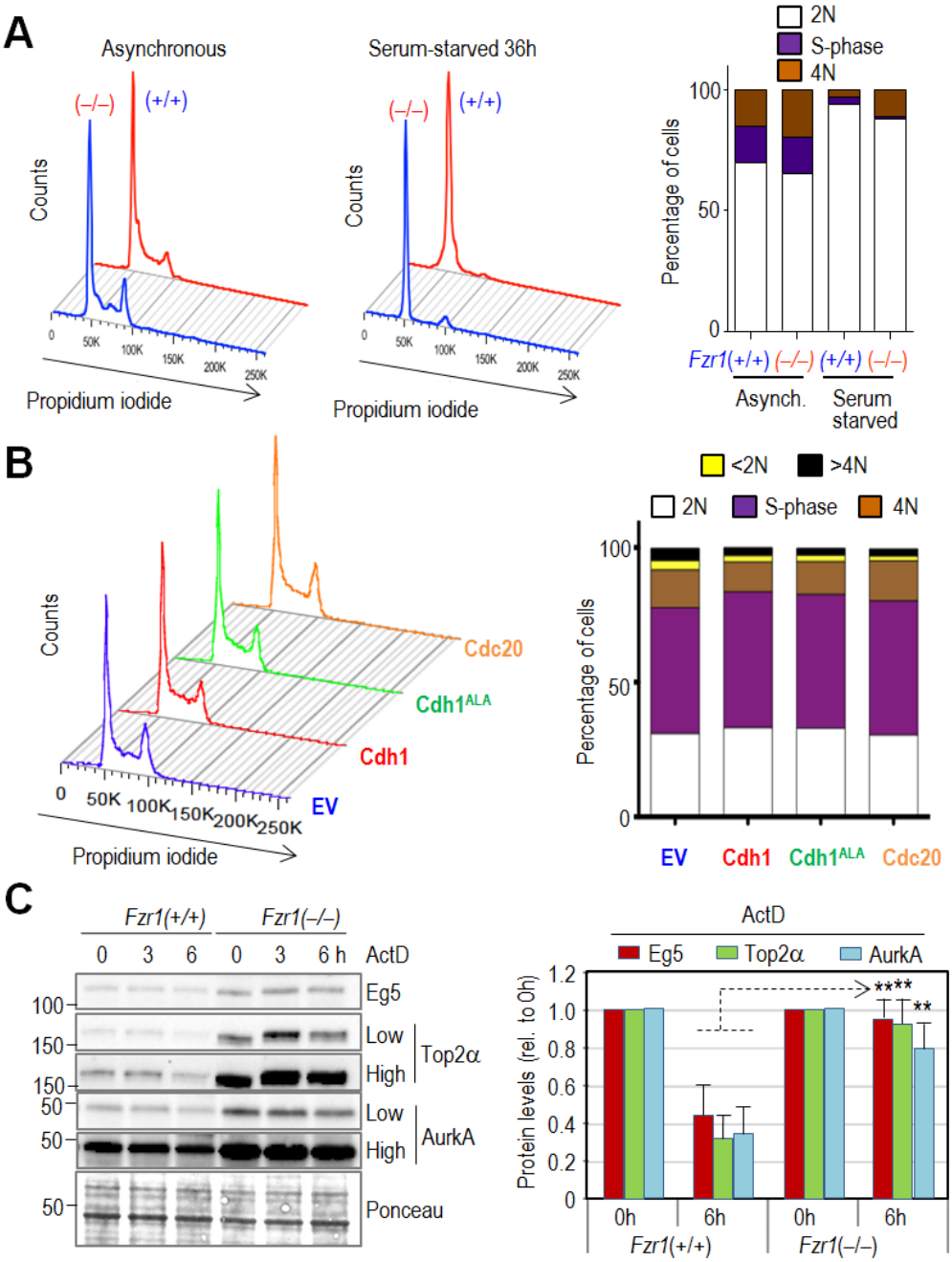

Figure S2. Cell Cycle profiles of cells deficient or overexpressing Cdh1 and stability of substrates upon treatment with actinomycin D (Related to Figs. 1-3). A, Cell cycle profiles of Cdh1-wild-type or Cdh1-null cells in the conditions used for the proteomic analysis. Note that Cdh1-null cells usually display increased 4N content due to the presence of tetraploid/binucleated cells. Histogram indicates representative average percentage of 2N cells (G0/G1), intermediate 2N-4N content (S-phase) or 4N (G2/M or tetraploid). B, Cell cycle profile of 293T cells after the expression of the indicated proteins or the empty vector (EV). The histogram represents the quantification of the percentage of cells in the different phases of the cell cycle in the previous assay. C, Protein stability of the indicated molecules in the presence of Actinomycin D (ActD) in Cdh1-null and control cells. Signals after low or high exposure are indicated for Aurora A and Top2α. The quantification of protein levels at 0 and 6 h after the addition of ActD is shown in the histogram. Data indicate mean ± SEM in two separate assays. **, p<0.01, Student's t-test.

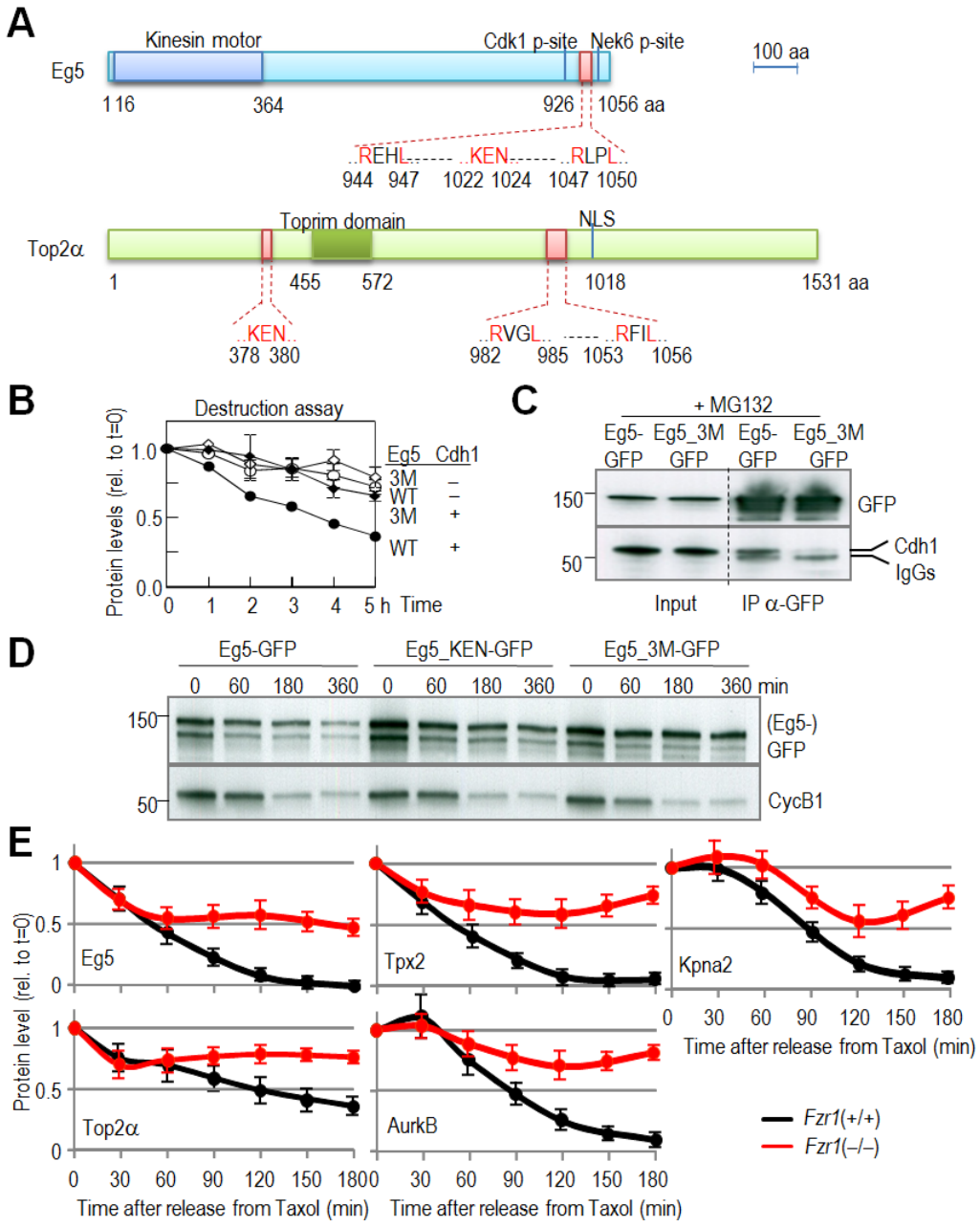

Figure S3. KEN and D-boxes in Eg5 and Top2α and kinetics of substrates in Cdh1-null cells. (related to Figs. 3-4) A, Schematic representation of human Eg5 and Top2α domains including putative KEN and D-boxes. Residues in red were mutated to alanine to generate stable proteins (3M mutants). B, Quantification of the destruction assay in Fig. 3H. Both the upper and lower (likely a prematurely terminated or partly cleaved product) bands in Fig. 3H show a similar kinetics. Only the upper band is quantified in the plot. Error bars, SEM from three independent experiments. C, Co-immunoprecipitation studies in 293T cells expressing Eg5-GFP or Eg5_3M-GFP fusion proteins. Protein extracts were immunoprecipitated with antibodies against GFP and the endogenous Cdh1 was detected in the presence of the proteasome inhibitor MG132. D, Protein levels of the exogenous Eg5-GFP fusion protein at different time points after a release from nocodazole. Eg5-KEN-GFP is mutated in the KEN box whereas Eg5_3M-GFP contains mutations in the KEN and two putative D-boxes. E, Comparative quantification of the levels of the indicated proteins after release from taxol in Cdh1-null [*Fzr1*(–/–)] or control [*Fzr1*(+/+)] MEFS. Values (mean ± SEM) were normalized to the amount of protein at t=0 (in the presence of taxol).

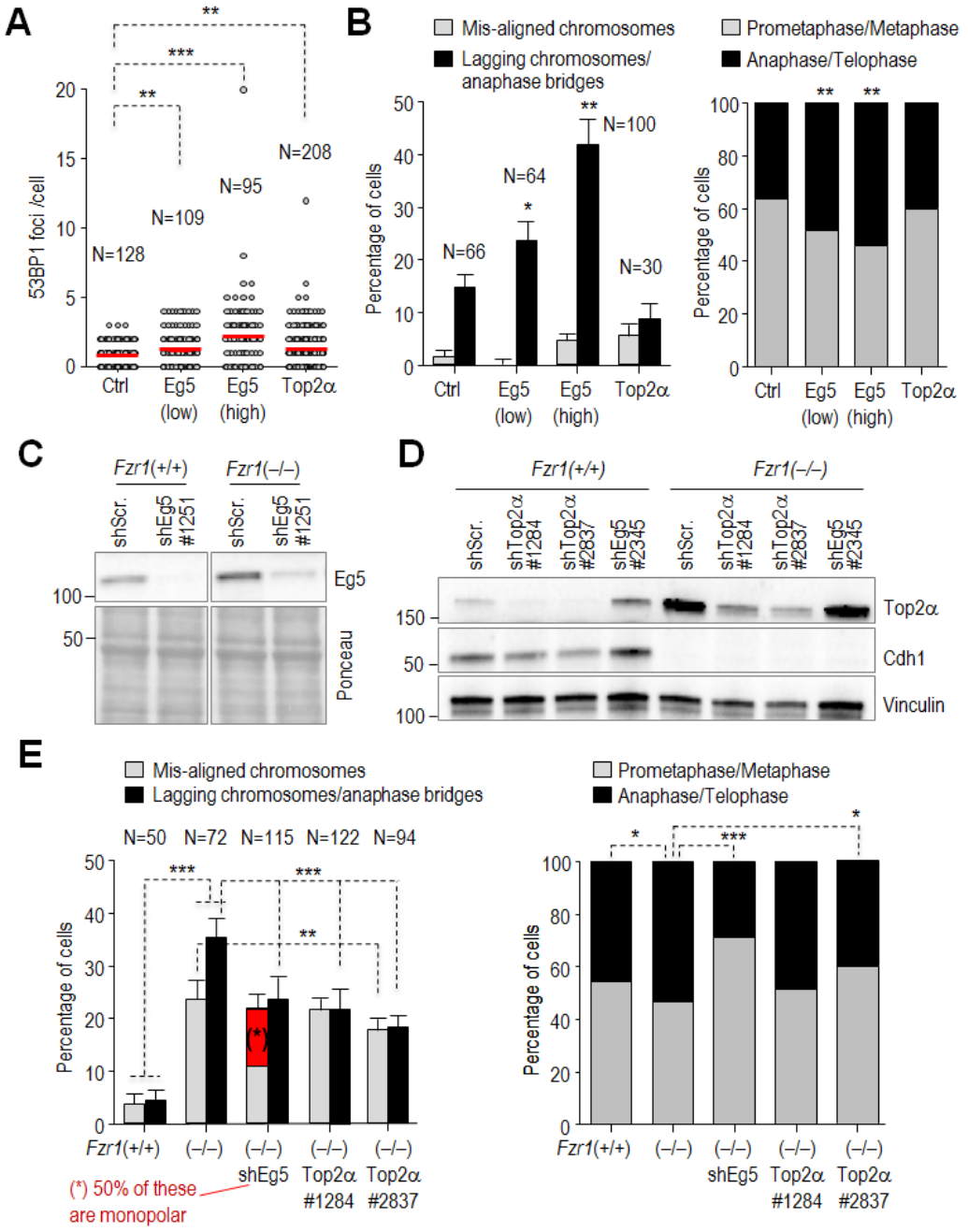

Figure S4. Effect of Eg5 and Top2α levels in genomic instability (related to Fig. 4). A, U2OS cells were transfected with Eg5 (low or high concentration) or Top2α and the number of 53BP1 foci was scored by immunofluorescence. Means are indicated by a red bar. N, number of cells. B, Mitotic aberrations were scored by immunofluorescence with antibodies against α-tubulin and DAPI to stain DNA. Data represent percentage of mitotic cells (mean ± SEM in three experiments). C-D, Downregulation of endogenous Eg5 (C) or Top2α (D) after transfection of Cdh1-null [*Fzr1*(–/–)] or control [*Fzr1*(+/+)] MEFs with short hairpin interfering RNAs (shRNAs) against these molecules. E, Mitotic aberrations (mean ± SEM in three experiments) in wild-type or Cdh1-null cells after knock-down of Eg5 or Top2α with the indicated shRNAs. N, number of cells. *, p<0.05; **, p<0.01; ***, p<0.001 (Student's t-test).

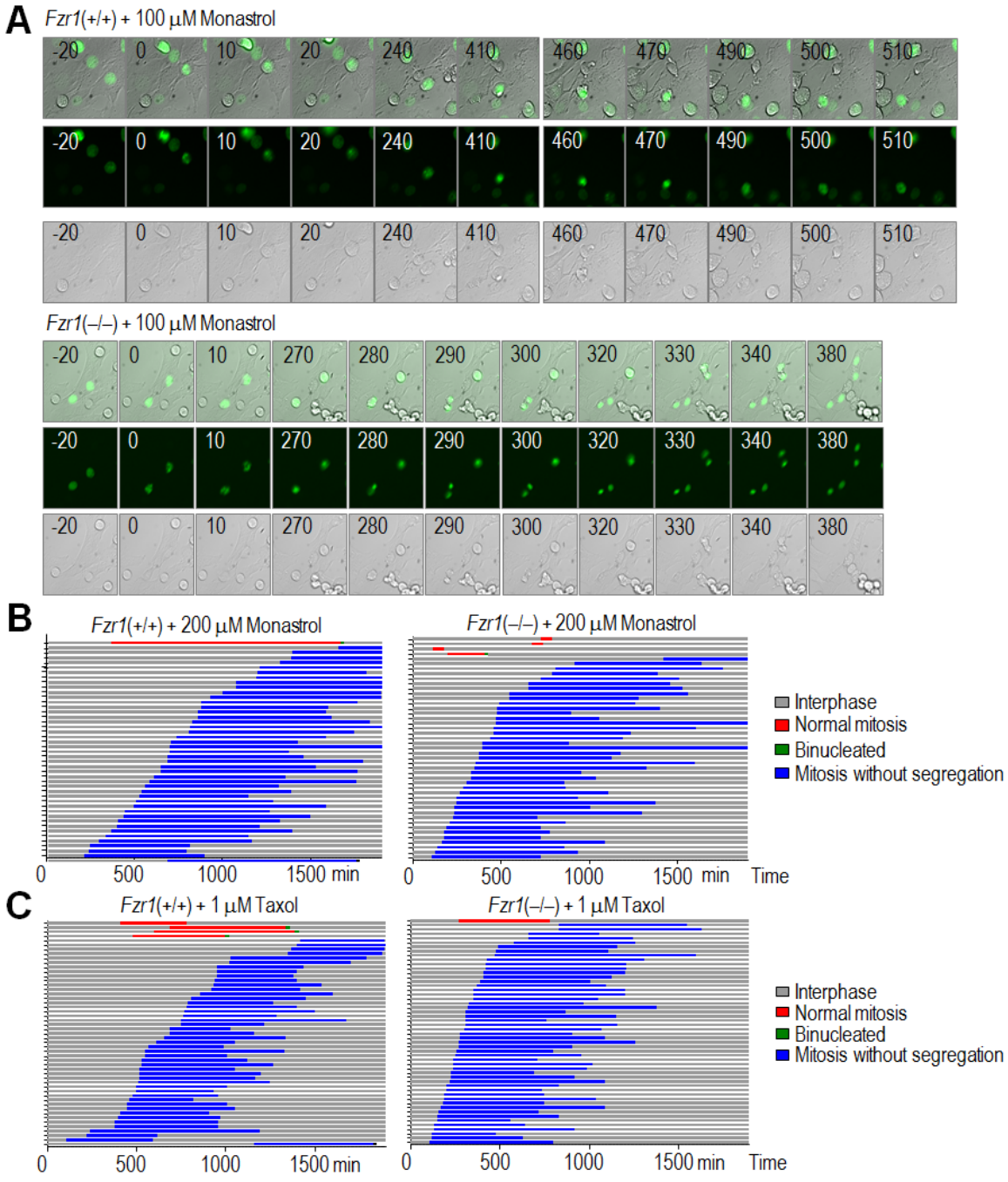

Figure S5. Effect of monastrol or taxol in Cdh1-null [*Fzr1*(–/–)] or wild-type [*Fzr1*(+/+)] cells (related to Fig. 5). A, Extended version from Figure 6B. Scale bars, 10 μM. B, Effect of increased (200 μM) dose of monastrol in wild-type or Cdh1-null cells, showing that the resistance of Cdh1-null cells to monastrol is dose-dependent. C, Effect of taxol in wild-type and Cdh1-null cells showing that lack of Cdh1 does not result in resistance to this microtubule poison.

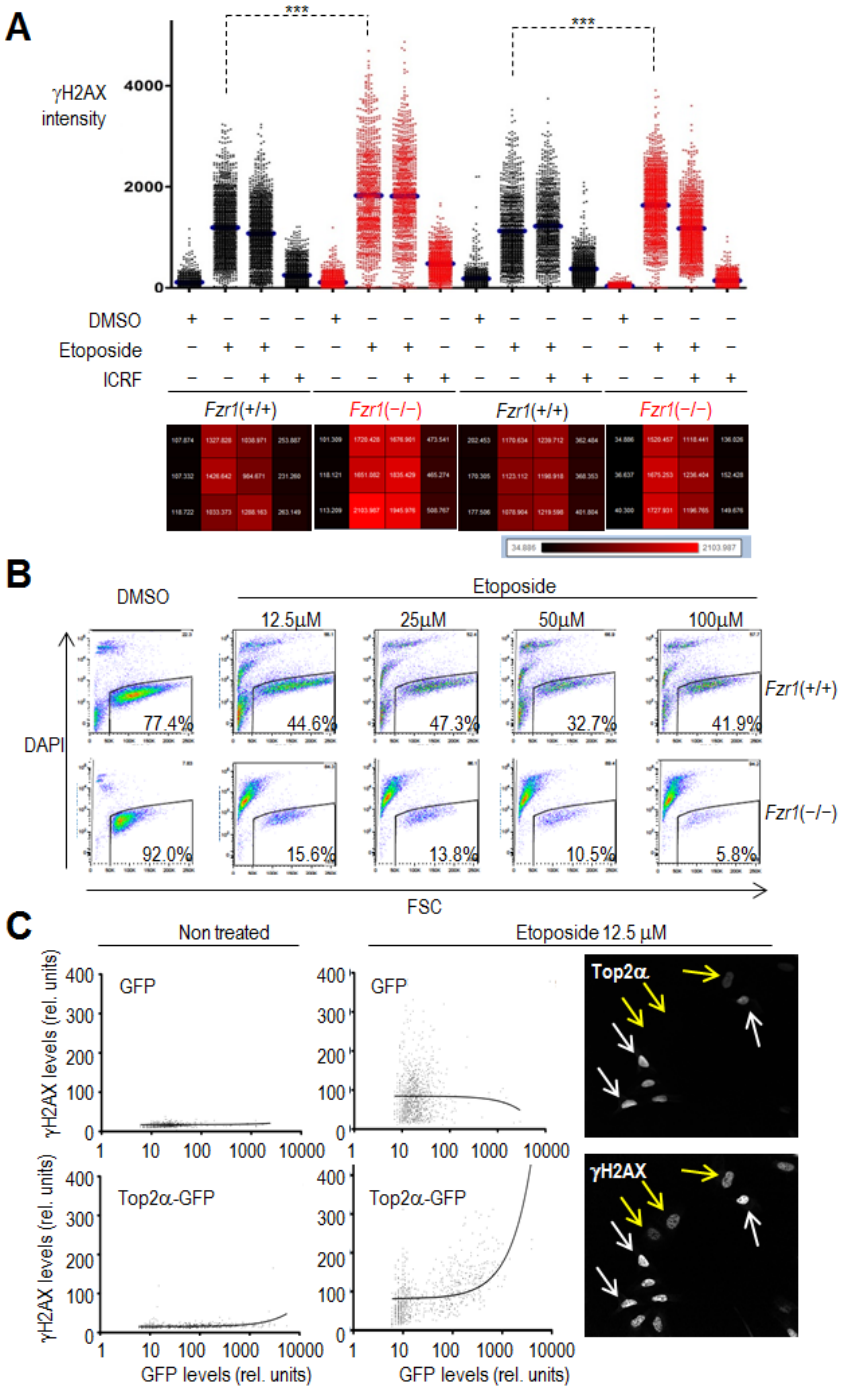

Figure S6. Effect of etoposide in Cdh1-null and control cells (related to Fig. 6). A, Quantification of phosphorylation of H2AX (γH2AX intensity per cell) after treatment of Cdh1-null or control cells with etoposide or ICRF-193. Please note that etoposide and ICRF-193 were added at the same time and, in these conditions, the addition of ICRF-193 is not efficient in preventing DNA damage induced by etoposide. B, Quantification of the lethal effect of etoposide at the indicated doses in Cdh1-null or control cells. The percentage of live cells (negative for DAPI) is indicated in each condition. Data show a representative assay of three independent experiments. C, γH2AX intensity per cell after overexpression of GFP or Top2α-GFP, in the absence or presence of the indicated dose of etoposide. Lines indicate regression analysis of the data. Pictures on the right represent levels of γH2AX in cells positive (white arrows) or negative (yellow arrows) for Top2α overexpression.

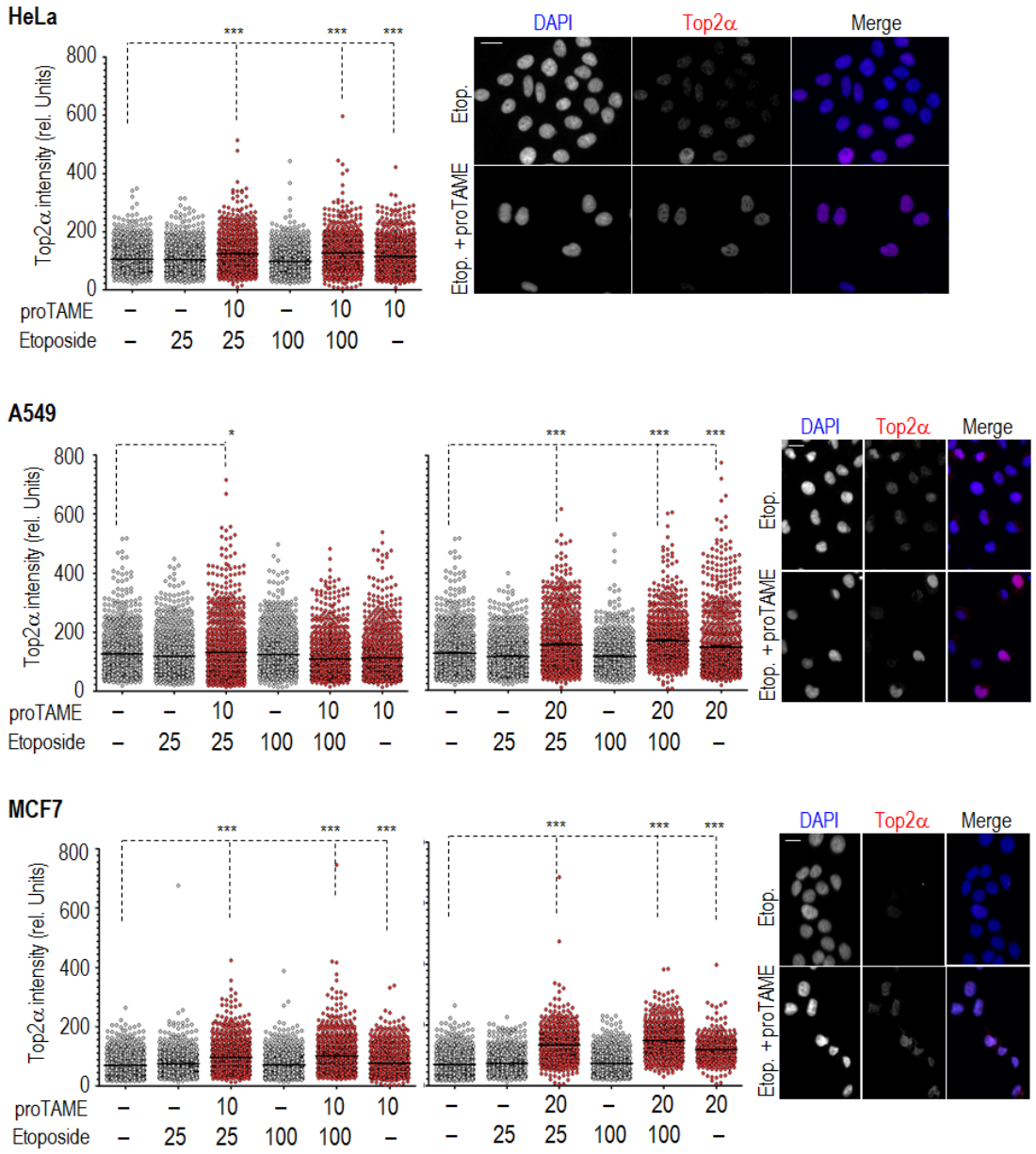

Figure S7. Protein levels of Top2α after inhibition of the APC/C in human cell lines (related to Fig. 7). Quantification of Top2α levels in HeLa, A549 or MCF7 cells treated with the indicated dose of proTAME or etoposide (μM). Representative images of cells treated with 25 μM etoposide or 25 μM etoposide + 10 μM proTAME (HeLa) or 25 μM etoposide + 20 μM proTAME (A549 and MCF7) are shown. Top2α is in red and DAPI in blue. Scale bars, 10 μM. At least 4000 cells per condition were quantified in these assays and only 1000 are represented in the plots for clarity. ***, $p<0.001$; Student's t-test.

Supplementary Tables

Table S1. Known APC/C substrates identified in our work (related to Table 1 and Figs 1-2).

Symbol	Uniprot	Description	Asynchr. Log*	G0 Log*	Brains Log*	Reference
Anln	Q8K298	Actin-binding protein anillin	1.668	0.983	nd	(Zhao & Fang, 2005)
Aurka	P97477	Aurora kinase A	nd	0.225	nd	(Taguchi et al, 2002) (Littlepage & Ruderman, 2002)
Aurkb	O70126	Aurora kinase B	0.991	nd	2.355	(Stewart & Fang, 2005) (Nguyen et al, 2005)
Brsk2	Q69Z98	Serine/threonine-protein kinase BRSK2	nd	nd	0.188	(Li et al, 2012)
Ccna2	P51943	Cyclin-A2	nd	-0.44	nd	(den Elzen & Pines, 2001) (Geley et al, 2001)
Ccnb1	P24860	Ccnb1 protein	nd	0.136	nd	(Clute & Pines, 1999)
Cdk5	P49615	Cyclin-dependent kinase 5	nd	0.085	-0.03	(Zhang et al, 2012)
Ckap2	Q3V1H1	Cytoskeleton-associated protein 2	2.116	1.024	0.845	(Seki & Fang, 2007) (Hong et al, 2007)
Dnmt1	P13864	DNA (cytosine-5)-methyltransferase 1	nd	0.03	-0.18	(Ghoshal et al, 2005)
Fan1	Q69ZT1	Fanconi-associated nuclease 1	-0.15	nd	nd	(Lai et al, 2012)
FoxM1	O08696	Forkhead box protein M1	nd	nd	-0.05	(Park et al, 2008)
Gls	D3Z7P3-2	Isoform 2 of Glutaminase kidney isoform, mitochondrial	nd	-0.37	-0.28	(Colombo et al, 2011)
Gtse1	Q8R080	G2 and S phase-expressed protein 1	nd	0.794	nd	(Pfleger & Kirschner, 2000)
Hmmr	Q00547	Hyaluronan mediated motility receptor	0.27	nd	nd	(Song & Rape, 2010)
Iqgap1	Q9JKF1	Ras GTPase-activating-like protein IQGAP1	0.877	-0.01	-0.19	(Ko et al, 2007)
Kif22	Q3V300	Kinesin-like protein KIF22	1.322	nd	nd	(Feine et al, 2007)
Mapk9	Q9WTU6	Isoform Alpha-1 of Mitogen-activated protein kinase 9	nd	-0.07	nd	(Gutierrez et al, 2010)
Mcl1	P97287	Induced myeloid leukemia cell differentiation protein Mcl-1 homolog	nd	-0.06	nd	(Harley et al, 2010)
RacGAP1	Q9WVM1	Rac GTPase-activating protein 1	0.33	nd	nd	(Nishimura et al, 2013)
Ndc80	Q9D0F1	Kinetochore protein NDC80 homolog	nd	nd	0.654	(Li et al, 2011)
Neurod2	Q62414	Neurogenic differentiation factor 2	nd	nd	-0.24	(Yang et al, 2009)
Nusap1	Q9ERH4	Nucleolar and spindle-associated	nd	nd	2.377	(Song & Rape,

		protein 1				2010)
Rrm2	P11157	Ribonucleoside-diphosphate reductase subunit M2	nd	0.255	-0.08	(Chabes et al, 2003)
Skp2	Q9Z0Z3	S-phase kinase-associated protein 2	nd	nd	0.283	(Bashir et al, 2004)(Wei et al, 2004)
Tacc3	Q9JJ11	Transforming acidic coiled-coil-containing protein 3	nd	0.845	1.959	(Jeng et al, 2009)
Tpx2	A2APB8	Targeting protein for Xklp2	0.623	nd	nd	(Stewart & Fang, 2005)
Trrap	Q80YV3	Transformation/transcription domain-associated protein	-0.04	-0.01	0.07	(Ichim et al, 2013)
Ube2c	Q9D1C1	Ubiquitin-conjugating enzyme E2 C	nd	0.041	nd	(Williamson et al, 2009)
Ube2s	Q921J4	Ubiquitin-conjugating enzyme E2 S	1.59	0.11	nd	(Williamson et al, 2009)

* nd, not detected.

Table S2. Antibodies used in this work (related to Figs. 1-4,6,7,S2,S3,S4,S6,S8).

Antigen	Ig	Source	Clone	Cat Number	Dilution	Technique*
53BP1	Rabbit	Novus Biologicals		NB100-304	1:1000	IF
AurkA	Mouse	Becton Dickinson	4/IAK1	610938	1:25	IHC
AurkA	Mouse	Abcam		ab13824	1:500	WB
AurkB	Rabbit	Abcam		ab2254	1:100-1:200	IHC/WB
β-Catenin	Mouse	Sigma		C 7207	1:1500	WB
Cdc20/p55CDC	Rabbit	Santa Cruz Biotechnology		sc-8358	1:200	WB
Cdc27	Mouse	Abcam		ab10538	1:500	WB
Cdh1	Mouse	Neomarkers	CH01	MS-1116-P	1:200	WB
Cyclin B1	Mouse	Chemicon		MAB3684	1:1000	WB
Gapdh	Mouse	Sigma		G9545	1:10000	WB
GFP	Mouse	Roche		11814460001	1:2000	WB
Kif11/Eg5	Rabbit	Cytoskeleton		AKIN03	1:500-1:1000	WB/IF
Kpna2	Rabbit	Novus			1:500	WB
Phospho-Histone H2A.X (Ser139)	Mouse	Millipore	JBW301	05-636	1:1000	IF
Rock2	Rabbit	Santa Cruz Biotechnology	H-85	sc-5561	1:200	WB
Securin	Mouse	Abcam		ab3305	1:500	WB
Skp1 p19	Rabbit	Santa Cruz Biotechnology	H-163	sc-7163	1:200	WB
Top2α	Rabbit	TopoGEN		2011-1	1:500-1:1000	WB/IF
Tpx2	Rabbit	Lifespan Biosciences		LS-B146	1:250-1:1000	IHC, WB
	Rabbit	Hyman's lab (MPI-CBG)			1:500	IF
	Mouse	Abcam		ab32795	1:500	WB
Vinculin	Mouse	Sigma-Aldrich	hVIN1	V9131	1:3000	WB

* IF, Immunofluorescence; IHC, immunohistochemistry; WB, immunoblot

Table S3. Oligonucleotides used in this work against mouse sequences (related to Fig. 3).

Primer	Sequence
Top2α_Forward	5′ TGGTCAGTTTGGAACCAGGC 3′
Top2α_Reverse	5′ TCAGGCTCAACACGTTGGTT 3′
Kif11_Forward	5′ TGGCAGTGCGAAACAAAAGG 3′
Kif11_Reverse	5′ TCTGAGAAACACGAGCGGAC 3′
Gadd45a_Forward	5' GCTCAACGTAGACCCCGATA 3'
Gadd45a_Reverse	5' GTTCGTCACCAGCACACAGT 3'
Cdkn1a_Forward	5' GTGGGTCTGACTCCAGCCC 3'
Cdkn1a_Reverse	5' CCTTCTCGTGAGACGCTTAC 3'
Tpx2_Forward	5' CCTCACAGATGAGCGAATCA 3'
Tpx2_Reverse	5' TCTTCCCTTTGGACAGGTTG 3'
Gapdh_Forward	5' GCCACCCAGAAGACTGTGGATGGC 3'
Gapdh_Reverse	5' CATGATGGCCATGAGGTCCACCAC 3'

Supplementary References

Bashir T, Dorrello NV, Amador V, Guardavaccaro D, Pagano M (2004) Control of the SCF(Skp2-Cks1) ubiquitin ligase by the APC/C(Cdh1) ubiquitin ligase. *Nature* 428: 190-193

Clute P, Pines J (1999) Temporal and spatial control of cyclin B1 destruction in metaphase. *Nat Cell Biol* 1: 82-87

Colombo SL, Palacios-Callender M, Frakich N, Carcamo S, Kovacs I, Tudzarova S, Moncada S (2011) Molecular basis for the differential use of glucose and glutamine in cell proliferation as revealed by synchronized HeLa cells. *Proc Natl Acad Sci U S A* 108: 21069-21074

Chabes AL, Pfleger CM, Kirschner MW, Thelander L (2003) Mouse ribonucleotide reductase R2 protein: a new target for anaphase-promoting complex-Cdh1-mediated proteolysis. *Proc Natl Acad Sci U S A* 100: 3925-3929

den Elzen N, Pines J (2001) Cyclin A is destroyed in prometaphase and can delay chromosome alignment and anaphase. *J Cell Biol* 153: 121-136

Feine O, Zur A, Mahbubani H, Brandeis M (2007) Human Kid is degraded by the APC/C(Cdh1) but not by the APC/C(Cdc20). *Cell Cycle* 6: 2516-2523

Geley S, Kramer E, Gieffers C, Gannon J, Peters JM, Hunt T (2001) Anaphase-promoting complex/cyclosome-dependent proteolysis of human cyclin A starts at the beginning of mitosis and is not subject to the spindle assembly checkpoint. *J Cell Biol* 153: 137-148

Ghoshal K, Datta J, Majumder S, Bai S, Kutay H, Motiwala T, Jacob ST (2005) 5-Aza-deoxycytidine induces selective degradation of DNA methyltransferase 1 by a proteasomal pathway that requires the KEN box, bromo-adjacent homology domain, and nuclear localization signal. *Mol Cell Biol* 25: 4727-4741

Gutierrez GJ, Tsuji T, Chen M, Jiang W, Ronai ZA (2010) Interplay between Cdh1 and JNK activity during the cell cycle. *Nat Cell Biol* 12: 686-695

Harley ME, Allan LA, Sanderson HS, Clarke PR (2010) Phosphorylation of Mcl-1 by CDK1-cyclin B1 initiates its Cdc20-dependent destruction during mitotic arrest. *EMBO J* 29: 2407-2420

Hong KU, Park YS, Seong YS, Kang D, Bae CD, Park J (2007) Functional importance of the anaphase-promoting complex-Cdh1-mediated degradation of TMAP/CKAP2 in regulation of spindle function and cytokinesis. *Mol Cell Biol* 27: 3667-3681

Ichim G, Mola M, Finkbeiner MG, Cros MP, Herceg Z, Hernandez-Vargas H (2013) The histone acetyltransferase component TRRAP is targeted for destruction during the cell cycle. *Oncogene*

Jeng JC, Lin YM, Lin CH, Shih HM (2009) Cdh1 controls the stability of TACC3. *Cell Cycle* 8: 3529-3536

Ko N, Nishihama R, Tully GH, Ostapenko D, Solomon MJ, Morgan DO, Pringle JR (2007) Identification of yeast IQGAP (Iqg1p) as an anaphase-promoting-complex substrate and its role in actomyosin-ring-independent cytokinesis. *Mol Biol Cell* 18: 5139-5153

Lai F, Hu K, Wu Y, Tang J, Sang Y, Cao J, Kang T (2012) Human KIAA1018/FAN1 nuclease is a new mitotic substrate of APC/C(Cdh1). *Chin J Cancer* 31: 440-448

Li L, Zhou Y, Wang GF, Liao SC, Ke YB, Wu W, Li XH, Zhang RL, Fu YC (2011) Anaphase-promoting complex/cyclosome controls HEC1 stability. *Cell Prolif* 44: 1-9

Li R, Wan B, Zhou J, Wang Y, Luo T, Gu X, Chen F, Yu L (2012) APC/C(Cdh1) targets brain-specific kinase 2 (BRSK2) for degradation via the ubiquitin-proteasome pathway. *PLoS One* 7: e45932

Littlepage LE, Ruderman JV (2002) Identification of a new APC/C recognition domain, the A box, which is required for the Cdh1-dependent destruction of the kinase Aurora-A during mitotic exit. *Genes Dev* 16: 2274-2285

Nguyen HG, Chinnappan D, Urano T, Ravid K (2005) Mechanism of Aurora-B degradation and its dependency on intact KEN and A-boxes: identification of an aneuploidy-promoting property. *Mol Cell Biol* 25: 4977-4992

Nishimura K, Oki T, Kitaura J, Kuninaka S, Saya H, Sakaue-Sawano A, Miyawaki A, Kitamura T (2013) APC(CDH1) targets MgcRacGAP for destruction in the late M phase. *PLoS One* 8: e63001

Olsen JV, de Godoy LM, Li G, Macek B, Mortensen P, Pesch R, Makarov A, Lange O, Horning S, Mann M (2005) Parts per million mass accuracy on an Orbitrap mass spectrometer via lock mass injection into a C-trap. *Mol Cell Proteomics* 4: 2010-2021

Ong SE, Blagoev B, Kratchmarova I, Kristensen DB, Steen H, Pandey A, Mann M (2002) Stable isotope labeling by amino acids in cell culture, SILAC, as a simple and accurate approach to expression proteomics. *Mol Cell Proteomics* 1: 376-386

Park HJ, Costa RH, Lau LF, Tyner AL, Raychaudhuri P (2008) Anaphase-promoting complex/cyclosome-CDH1-mediated proteolysis of the forkhead box M1 transcription factor is critical for regulated entry into S phase. *Mol Cell Biol* 28: 5162-5171

Pfleger CM, Kirschner MW (2000) The KEN box: an APC recognition signal distinct from the D box targeted by Cdh1. *Genes Dev* 14: 655-665

Ross PL, Huang YN, Marchese JN, Williamson B, Parker K, Hattan S, Khainovski N, Pillai S, Dey S, Daniels S, Purkayastha S, Juhasz P, Martin S, Bartlet-Jones M, He F, Jacobson A, Pappin DJ (2004) Multiplexed protein quantitation in Saccharomyces cerevisiae using amine-reactive isobaric tagging reagents. *Mol Cell Proteomics* 3: 1154-1169

Seki A, Fang G (2007) CKAP2 is a spindle-associated protein degraded by APC/C-Cdh1 during mitotic exit. *J Biol Chem* 282: 15103-15113

Shevchenko A, Tomas H, Havlis J, Olsen JV, Mann M (2006) In-gel digestion for mass spectrometric characterization of proteins and proteomes. *Nat Protoc* 1: 2856-2860

Song L, Rape M (2010) Regulated degradation of spindle assembly factors by the anaphase-promoting complex. *Mol Cell* 38: 369-382

Stewart S, Fang G (2005) Anaphase-promoting complex/cyclosome controls the stability of TPX2 during mitotic exit. *Mol Cell Biol* 25: 10516-10527

Taguchi S, Honda K, Sugiura K, Yamaguchi A, Furukawa K, Urano T (2002) Degradation of human Aurora-A protein kinase is mediated by hCdh1. *FEBS Lett* 519: 59-65

Wei W, Ayad NG, Wan Y, Zhang GJ, Kirschner MW, Kaelin WG, Jr. (2004) Degradation of the SCF component Skp2 in cell-cycle phase G1 by the anaphase-promoting complex. *Nature* 428: 194-198

Williamson A, Wickliffe KE, Mellone BG, Song L, Karpen GH, Rape M (2009) Identification of a physiological E2 module for the human anaphase-promoting complex. *Proc Natl Acad Sci U S A* 106: 18213-18218

Yang Y, Kim AH, Yamada T, Wu B, Bilimoria PM, Ikeuchi Y, de la Iglesia N, Shen J, Bonni A (2009) A Cdc20-APC ubiquitin signaling pathway regulates presynaptic differentiation. *Science* 326: 575-578

Zhang J, Li H, Zhou T, Zhou J, Herrup K (2012) Cdk5 levels oscillate during the neuronal cell cycle: Cdh1 ubiquitination triggers proteosome-dependent degradation during S-phase. *J Biol Chem* 287: 25985-25994

Zhao WM, Fang G (2005) Anillin is a substrate of anaphase-promoting complex/cyclosome (APC/C) that controls spatial contractility of myosin during late cytokinesis. *J Biol Chem* 280: 33516-33524